Biophysical Journal Volume 76 January 1999 1–16

Biomolecular Electrostatics with the Linearized Poisson-Boltzmann Equation

Federico Fogolari,* Pierfrancesco Zuccato,*†, Gennaro Esposito,† and Paolo Viglino†

*Dipartimento Scientifico Tecnologico, University of Verona, 37100 Verona, and †Dipartimento di Scienze e Tecnologie Biomediche, Università di Udine, 33100 Udine, Italy

ABSTRACT Electrostatics plays a key role in many biological processes. The Poisson-Boltzmann equation (PBE) and its linearized form (LPBE) allow prediction of electrostatic effects for biomolecular systems. The discrepancies between the solutions of the PBE and those of the LPBE are well known for systems with a simple geometry, but much less for biomolecular systems. Results for high charge density systems show that there are limitations to the applicability of the LPBE at low ionic strength and, to a lesser extent, at higher ionic strength. For systems with a simple geometry, the onset of nonlinear effects has been shown to be governed by the ratio of the electric field over the Debye screening constant. This ratio is used in the present work to correct the LPBE results to reproduce fairly accurately those obtained from the PBE for systems with a simple geometry. Since the correction does not involve any geometrical parameter, it can be easily applied to real biomolecular systems. The error on the potential for the LPBE (compared to the PBE) spans few kT/q for the systems studied here and is greatly reduced by the correction. This allows for a more accurate evaluation of the electrostatic free energy of the systems.

INTRODUCTION

Electrostatics plays a key role in biological processes (Honig and Nicholls, 1995; Davis and McCammon, 1990; Davis et al., 1991). The binding of small electrolytes to a biomolecule in solution is kinetically driven by the electrostatic field generated by the molecule and is highly correlated with the electrostatic potential at the surface of the molecule. In many cases the nonobvious dependence of the kinetic constants of association between an enzyme and a substrate on the solution ionic conditions or kinetic pathways could be elucidated by analysis of the electrostatic fields in solution (Gilson et al., 1994; Sharp et al., 1987). Inspection of many molecular complexes has shown a high degree of complementarity in the electrostatic properties of the contacting surfaces (Honig and Nicholls, 1995). The electrostatic properties of biomolecular systems are influenced by pH and ionic conditions. The extent to which a group is ionized depends on the electrostatic potential generated at that site by the molecule (e.g., Antosiewicz et al., 1994). The ionization state of a biomolecule is in turn crucial for its function and stability.

The methods that have been used to simulate electrostatics in biological systems may be broadly classified into those which simulate explicitly all molecules of the system, including salts and solvent, which are by far the more demanding, and those which simulate the solvent and salts through a continuum model. Among the latter, the Poisson-Boltzmann equation (PBE) has been widely and successfully used. In recent years refined theoretical and numerical tools have been developed to apply the PBE to biomolecular systems (Gilson et al., 1987; Sharp and Honig, 1990; Zhou, 1994; Madura et al., 1995) and a large number of results have been achieved (Madura et al., 1994; Honig and Nicholls, 1995).

The reliability of the PBE has been tested for a few models and real systems by means of more sophisticated methods, such as Monte Carlo or hypernetted chain simulations (Fixman, 1979; Murthy et al., 1985, Jayaram and Beveridge, 1996).

The Poisson-Boltzmann equation was first put forward more than 80 years ago by Gouy (1910) and few years later by Chapman (1913). The equation was obtained either by equating to zero the forces acting on a microscopic volume of the ionic solution (Gouy, 1910) or by equating the chemical potential throughout the solution (Chapman, 1913). The same approaches have been followed by other researchers in the field of colloid chemistry (Derjaguin and Landau, 1941; Verwey and Overbeek, 1948) and electrocapillarity (Grahame, 1947).

Except for the simple planar geometry in the presence of symmetrical electrolytes (Gouy, 1910; Chapman, 1913) and the cylindrical geometry in the absence of added salt (Alfrey et al., 1951; Lifson and Katchalsky, 1954; Katchalsky, 1971), no analytical solution is available. Debye and Hückel (1923), who developed the PBE aiming at explicit calculation of the free energy for an ionic system, noticed that under usual experimental conditions the equation can be linearized to a good degree of accuracy for the computation of various thermodynamic quantities.

Although a number of software packages allow for the solution of the nonlinear PBE (Gilson et al., 1987; Madura et al., 1995), it is often mandatory to employ the linear approximation to reduce computation time. Depending on

Received for publication 18 March 1998 and in final form 17 July 1998.

Address correspondence and reprint requests to Dr. Federico Fogolari, Dipartimento Scientifico Tecnologico, Facolta' di Scienze MM. FF. NN., Ca' Vignal 1, Strada Le Grazie, 37100 Verona, Italy. Tel.: 39 45 8098949; Fax: 39 45 8098929; E-mail: federico@nmr.sci.univr.it.

0006-3495/99/01/01/16 $2.00

the system, the solution of the nonlinear PBE takes usually more than twice the time needed to solve its linear version. Moreover, since the electrostatic potential in the linear PBE (LPBE) is the superposition of the electrostatic potentials of each partial charge on the molecule, for all those applications where a charge is modified without altering the molecular shape (like in idealized protonation or deprotonation of an ionizable group), additional computing time is saved (Antosiewicz et al., 1994).

There are at least four major applications of the PBE and its linear form:

(1) calculation of the electrostatic potential at the surface of a biomolecule, which is expected to give information about the concentration of small charged solutes in the neighborhood of the molecule and whose inspection may suggest docking sites for biomolecules;
(2) calculation of the electrostatic potential outside the molecule, which is expected to give information on the free energy of interaction of small molecules at different positions in the surrounding of the molecule. The electrostatic field is therefore used in Brownian dynamics simulations employing the so-called test charge approximation;
(3) calculation of the free energy of a biomolecule or of different states of a biomolecule which gives information on the stability of a biomolecule or of its different states (Sharp and Honig, 1990); and
(4) calculation of the electrostatic field to derive mean forces to be added in standard molecular dynamics calculations (Gilson et al., 1993).

It is of interest, therefore, to investigate the limits of applicability of the LPBE for biomolecular systems and for these applications.

In the present study we address some of these issues, in particular:

(1) How accurate are the potentials derived via the LPBE for typical biomolecular systems?
(2) Is it possible to correct the biomolecular potential maps obtained via the LPBE in order to reproduce more faithfully the PBE results?
(3) How accurate is the free energy computed in the linear approximation?
(4) Is it possible to employ the LPBE potential to reach a better approximation of the PBE free energy?

We first compare the results obtained from the LPBE and PBE for systems with a simple geometry (i.e. the plane, the cylinder, and the sphere). Because the PBE for these shapes is characterized by a parameter (Gueron and Weisbuch, 1980) ($m = 0, 1, 2$ for the plane, the cylinder, and the sphere, respectively) we can heuristically set this parameter to intermediate values which could represent behaviors in intermediate cases.

Then we examine some biological systems and see how well the considerations for the simple shapes translate to these highly asymmetrical systems.

THEORY

The PBE

In the Poisson-Boltzmann approach the macromolecule is treated as a low dielectric cavity with embedded atomic partial charges. The dielectric constant of the cavity is typically set between 2 and 4 to take into account electronic polarization and the limited flexibility of the macromolecule (Sharp et al., 1992; Gilson and Honig, 1986). The effects of the solvent molecules, whose motions are much faster than those of the molecule and the ions, are taken into account on average through a continuum of high dielectric constant (McCammon and Harvey, 1987).

The average electrostatic potential ($\bar{U}$) is determined by the charge density embedded in the molecule (ρ^{f}) and by the average charge density due to the mobile ions $\bar{\rho}^{\mathrm{m}}$, via the Poisson equation:

$$\vec{\nabla} \cdot (\epsilon \vec{\nabla} \bar{U}) = -4\pi \bar{\rho}^{\mathrm{m}} - 4\pi \rho^{\mathrm{f}} \tag{1}$$

where ϵ is the position-dependent dielectric constant and all terms are expressed in centimeter gram second-electrostatic units. The charge density $\bar{\rho}^{\mathrm{m}}$ can be expressed in terms of the bulk concentrations and a potential of mean force:

$$\bar{\rho}^{\mathrm{m}} = \sum_{\mathrm{i}} c_{\mathrm{i}}^{\infty} z_{\mathrm{i}} q \exp\left(\frac{-w_{\mathrm{i}}}{kT}\right) \tag{2}$$

where c_{i}^{∞} is the concentration of ion i at an infinite distance from the molecule (or at any reference position where the potential of mean force w_{i} is set to zero), z_{i} is its charge number, q is the proton charge, k is the Boltzmann constant and T is the temperature.

The key assumptions to obtain the PBE are that the potentials of mean force are given by $w_{\mathrm{i}} = z_{\mathrm{i}} q U$ and that U is equal to the average electrostatic potential $\bar{U}$:

$$\vec{\nabla} \cdot (\epsilon \vec{\nabla} U) = -4\pi \sum_{\mathrm{i}} c_{\mathrm{i}}^{\infty} z_{\mathrm{i}} q \exp\left(\frac{-z_{\mathrm{i}} q U}{kT}\right) - 4\pi \rho^{\mathrm{f}} \tag{3}$$

When the term $(z_{\mathrm{i}} q U/kT) \ll 1$ the exponential can be expanded in a Taylor series, retaining only the first two terms. Due to electroneutrality, $\Sigma_{\mathrm{i}} c_{\mathrm{i}}^{\infty} z_{\mathrm{i}} q = 0$, the LPBE is obtained:

$$\vec{\nabla} \cdot (\epsilon \vec{\nabla} U) = \left(\sum_{\mathrm{i}} 4\pi c_{\mathrm{i}}^{\infty} \frac{z_{\mathrm{i}}^2 q^2}{kT}\right) U - 4\pi \rho^{\mathrm{f}} \tag{4}$$

The most serious inconsistency of the PBE (Eq. 3) stems from the lack of reciprocity, i.e., different distributions are obtained for an ion pair by switching the definition of the central ion (Onsager, 1933; Fowler and Guggenheim, 1939). For some time this was regarded as an issue in favor of linearization.

Electrostatic free energy from the PBE

The electrostatic free energy for the hypothetical process of charging a sphere, organizing and charging the ionic atmo-

sphere was earlier calculated according to the adiabate principle (Onsager, 1933; Verwey and Overbeek, 1948) where the free energy is obtained from the charging integral:

$$\Delta G^{\mathrm{el}} = \int_0^{\tau} qU(\tau')d\tau' \tag{5}$$

where τq is the final charge on the sphere.

Another expression for the free energy of the process of charging the system, put forward by Marcus (1955), employs standard expressions for the chemical potential of solute molecules and is closely related to the expression we give below.

Sharp and Honig (1990) and, independently, Reiner and Radke (1990) derived the electrostatic free energy from a variational principle. They considered the PBE and built the Euler-Lagrange functional, which is extremized by the solution of the PBE. With an appropriate choice of multiplicative and additive constants, this functional could easily be interpreted as the free energy of the system.

The expression for the free energy is

$$\Delta G^{\mathrm{el}} = \int_{\mathrm{V}} \left(kT \sum_{\mathrm{i}} c_{\mathrm{i}}^{\infty} \left[1 - \exp\left(\frac{-z_{\mathrm{i}} qU}{kT} \right) \right] + \rho^{\mathrm{f}} U - \frac{\epsilon(\tilde{\nabla} U)^2}{8\pi} \right) \mathrm{d}V \tag{6}$$

though other forms, not involving derivatives of the potential, may be derived by exploiting the basic relationships $\int_{\mathrm{V}} (\epsilon(\nabla U)^2/8\pi)\mathrm{d}V = \int_{\mathrm{V}} (\rho U/2)\mathrm{d}V$ and $c_{\mathrm{i}} = c_{\mathrm{i}}^{\infty} \exp(-z_{\mathrm{i}} qU/kT)$ (Sharp and Honig, 1990).

The derivation faces several problems, however, including the paradoxical observation that the functional is not minimized but maximized. Nevertheless, it is possible to show that a proper free energy functional, defined by combining standard thermodynamics and the usual Poisson-Boltzmann approximations, is minimized by the ionic distribution obtained via the PBE (Fogolari and Briggs, 1997). Zhou (1994) showed that the free energy given by Eq. 6 may be alternatively obtained by a standard charging process (Eq. 5), and that the free energy is independent of the charging pathway.

For practical reasons we may rewrite the electrostatic free energy in terms of different contributions due to the electrostatic energy obtained by integrating $\rho U/2$ over two regions entailing the fixed (ΔG^{ef}) and mobile charges (ΔG^{em}), and the entropic (for a discussion of the entropy in electrostatic systems see Sharp, 1995) free energy of mixing of mobile species (ΔG^{mob}) and solvent (ΔG^{solv}),

$$\Delta G^{\mathrm{el}} = \Delta G^{\mathrm{ef}} + \Delta G^{\mathrm{em}} + \Delta G^{\mathrm{mob}} + \Delta G^{\mathrm{solv}} \tag{7}$$

where the different contributions read:

$$\Delta G^{\mathrm{ef}} = \int_{\mathrm{V}} \frac{\rho^{\mathrm{f}} U}{2} \mathrm{d}V \tag{8}$$

$$\Delta G^{\mathrm{em}} = \int_{\mathrm{V}} \frac{\sum_{\mathrm{i}} c_{\mathrm{i}} z_{\mathrm{i}} qU}{2} \mathrm{d}V \tag{9}$$

$$\Delta G^{\mathrm{mob}} = kT \int_{\mathrm{V}} \sum_{\mathrm{i}} c_{\mathrm{i}} \ln \frac{c_{\mathrm{i}}}{c_{\mathrm{i}}^{\infty}} \mathrm{d}V \tag{10}$$

$$\Delta G^{\mathrm{solv}} = kT \int_{\mathrm{V}} \sum_{\mathrm{i}} c_{\mathrm{i}}^{\infty} \left[1 - \exp\left(\frac{-z_{\mathrm{i}} qU}{kT} \right) \right] \mathrm{d}V \tag{11}$$

The latter three terms may be further grouped into a single term to indicate the outer space contribution to the free energy density integral:

$$\Delta G^{\mathrm{out}} = \Delta G^{\mathrm{em}} + \Delta G^{\mathrm{mob}} + \Delta G^{\mathrm{solv}} \tag{12}$$

This decomposition of the free energy does not correspond to any thermodynamic pathway but, in fact, it is closely related to the way software packages compute the electrostatic free energy. Misra et al. (1994) considered a thermodynamic pathway for charging the molecule and organizing and charging the ionic atmosphere that allows identification of the non-salt-dependent contribution to the free energy of the system (ΔG^{ns}), the contribution arising from the ionic atmosphere interaction with the molecule (ΔG^{im}), the contribution from the ion-ion interactions (ΔG^{ii}), and the contribution from the entropy cost of organizing the ionic atmosphere around the solute (ΔG^{org}).

The relationship of such a decomposition with the one given above (Eq. 7) is straightforward and is reported in Fogolari et al. (1997).

In the LPBE approach the only term contributing electrostatic free energy is ΔG^{ef} (Sharp and Honig, 1990) up to the order of the linear approximation, though some simple corrections may be devised, as we discuss below.

Applications of the LPBE to biomolecular systems

It is generally recognized that when $(qU/kT) \ll 1$ the PBE can be approximated by the LPBE which results from the approximation $\sinh(qU/kT) \approx qU/kT$. But it is common experience, at least in biomolecular simulations, that the solution of the LPBE is close to the solution of the PBE even when qU/kT at the molecular surface is in the range of 1 to 2, although in such cases the hyperbolic sine is 20% to 80% larger than the corresponding linear approximation. For higher potentials, even when the potential is several kT/q, the solutions of the LPBE and the PBE are not as dramatically distant as $\sinh(qU/kT)$ and qU/kT are.

The LPBE solution is usually larger than the PBE one. For centrosymmetrical ions in symmetrical solutions Gronwall, La Mer, and Sandved (1928) have given a series correction to the solution of the LPBE, but such rather involved expansion is of little use when dealing with

irregularly shaped molecules possessing uneven charge distributions.

Before approaching complex biomolecular systems we consider systems with a simple geometry, which can be highly idealized models for proteins, nucleic acids, and membranes. For these systems we find a general correction rule that brings the LPBE potential close to the PBE potential at the surface. We also define some simple rules to derive free energies from the solution of the LPBE, which include contributions to the free energy integral from the outer volume of the molecule.

Systems with a simple geometry

The PBE and LPBE have been numerically solved and compared for systems with a simple geometry (SSG) where the corresponding equations are dependent on either one or two variables, depending on the symmetry of the system. Much attention has been given to planar, cylindrical, and spherical shapes (Gueron and Weisbuch, 1980; Stigter 1978) and, more recently, to spheroidal geometries (Yoon and Kim, 1989; Hsu and Liu, 1996a,b).

Usually the equations are solved for simple boundary conditions, like constant surface charge or potential, or for a mix of these. This is an excellent approximation in the fields of colloid chemistry, where the surface charge is often controlled via ionizable groups sensitive to changes in pH, or electrocapillarity, where the electrode potential is externally controlled. However, it is bound to give only a very rough picture of biomolecules.

Moreover, SSG are very rough representations of real biomolecules. For instance the cylindrical model does an excellent job for regular biopolymers like DNA, but it is very difficult to model proteins with spheres or ellipsoids of constant charge. A more sophisticated approach was proposed by Kirkwood (1934), but still it appears too simplistic to represent real biomolecules. Nevertheless, SSG may be easily and extensively studied and conclusions reached about these systems may apply to complex systems. For these reasons SSG have received much attention in the past as model systems.

The relevant equations and definitions for SSG are reported in Appendix A. It is apparent that the solution of the PBE and all the derived thermodynamic quantities depend on the boundary conditions which may be imposed through the reduced electric field $\phi'(x_0)$ at the surface position expressed in Debye lengths. These are in turn determined by the interplay of three relevant length scales: the radius of curvature, the Debye length, and the electric field scale length, defined in Appendix B. Previous results obtained on SSG, summarized in Appendix B, showed similarities between the behavior of the PBE solution for systems with different geometry and showed that for all systems the ratio λ_D/Θ appears critical for the applicability of the linearization. Rather than studying the solution of the PBE, which depends on the shape and on the radius of curvature, we reasoned that the relationship between the solutions of the LPBE and the PBE should depend, in addition to the absolute values they can take, on the parameter λ_D/Θ itself. In particular they should be coincident when $(\lambda_D/\Theta) \gg 1$, whereas for $(\lambda_D/\Theta) \ll 1$ we have $\phi_{PBE} \approx 2 \ln(|\partial\phi_{PBE}/\partial x|_{x_0}|)$. Therefore we searched for a correction to be applied to the solution of the LPBE which depends only on the ratio λ_D/Θ, to recover the PBE solution. For its simple connection with the boundary conditions we rewrite λ_D/Θ in reduced units: $(\lambda_D/\Theta) = (2/\phi'(x_0))$, where the derivative is taken with respect to r/λ_D.

MATERIALS AND METHODS

Calculation protocols

For SSG the one-variable PBE and LPBE were solved numerically using an adaptive Runge-Kutta fourth-order algorithm (Press et al., 1990). Tentative values were put forward for the value of the potential at the surface and the behavior of the potential or its derivative at ≥5 Debye lengths from the surface was checked. The guess value for the surface potential was reset until the reduced potential and its derivative were <0.005 at 5 Debye lengths. All thermodynamic quantities were then obtained using the discretized analogs of the equations reported in the theory section.

All biomolecular simulations were performed with the software package UHBD (Madura et al., 1995) using standard procedures. The calculations employed a grid of 110 × 110 × 110 points with a grid mesh of 1.37 Å and one focusing step for a final grid mesh of 0.51 Å. In all calculations the dielectric constants of the solvent and solute molecules were 78 and 4, respectively. The radius of the ions was 2.0 Å and the solvent probe radius was 1.4 Å.

For the test of the electrostatic potential inside the molecule we used a grid of 110 × 110 × 110 points with a grid mesh of 1.0 Å in order to have all surface points inside the grid.

We have run a few tests on different conformers of amino acids in model dipeptide and tripeptide compounds studied by Fogolari et al. (1998) and on some anthracycline drugs studied by Baginski et al. (1997). In all these cases, studied at 150 mM ionic strength, the LPBE and the PBE gave virtually identical results.

We have chosen the following systems as test cases: a complex between the Antennapedia homeodomain with Cys 39 substituted by a serine (Antp C39S HD) (Billeter et al., 1993) and a stretch of 31 base pairs of DNA as a highly charged system with positive and negative regions of irregular shape (for details on the construction of the molecular model see Fogolari et al. (1997)), the isolated homeodomain which possesses an extended arm with positively charged residues as a highly positively charged mainly globular but irregularly shaped system, the isolated DNA as a highly charged cylindrical system and monomeric bovine β-lactoglobulin at pH 2, as a highly charged overall globular system. For the last system the most probable protonation state was obtained following the protocol of Antosiewicz et al. (1994) applied on the structure of the monomeric unit A, recently obtained by Sawyer and coworkers (Brownlow et al., 1996), but using the partial charges taken from the forcefield CHARMM (version 22) (Brooks et al., 1983). For this protein the presence of a stable core in the monomer with most native connectivities at pH 2 was established by Ragona et al. (1997) via NMR spectroscopy. Because in the most probable protonation state only few carboxylic groups are still deprotonated making the overall net charge positive and very high, we have decided to keep all the ionizable sites protonated, since in the present context this theoretical model is chosen only for the purpose of comparing the LPBE and PBE solutions.

Optimized parameters for liquid simulation charges and atomic radii (Jorgensen and Tirado-Rives, 1988, Pranata et al., 1991) were employed in the calculations on the homeodomain-DNA complex, and isolated DNA and homeodomain, while for β-lactoglobulin the set of CHARMM charges

and radii was used (Brooks et al., 1983). The temperature was set to 300 K. The net charge of the molecules is −47 for the homeodomain-DNA complex, −62 for the DNA, 15 for the homeodomain and 21 for β-lactoglobulin. β-lactoglobulin (2580 atoms) and homeodomain (790 atoms) have a radius of ~25 Å, while DNA (2754 atoms) is approximately a cylinder with radius 10 Å and length 100 Å. Thermodynamic quantities were computed from the output accessibility and potential maps. Surface points were obtained as the interfacial points in the solvent.

Computation times

Typically, 3800 to 6200 s were required by UHBD on a Silicon Graphics, Inc. (Mountain View, CA) O2, R5000, 180 MHz computer with 128 Mbytes RAM to solve the larger and focused grid. Corresponding times for the LPBE ranged from 1800–2600 s. Generating the corrected potential grid map and extracting thermodynamic quantities from the map takes <120 s, so that the correction procedure is negligible on the overall computation time. The generation of the potential inside the molecule, tested only for β-lactoglobulin (2580 atoms and 6328 interfacial points) takes ~200 s, but this time could be greatly optimized by properly selecting the interfacial points and possibly by choosing faster ways to solve Laplace's equation with Dirichlet boundary conditions.

RESULTS AND DISCUSSION

SSG

We have solved numerically the PBE and LPBE for a large number of boundary conditions and for different values of m (0, 0.4, 0.5, 0.8, 1.0, 1.2, 1.5, 1.6, and 2.0). Although noninteger values of m do not have a general physical counterpart, we expect these to represent intermediate cases between the three limiting simple shapes.

Surface electrostatic potentials

The plots of the solution of the PBE versus that of the LPBE at the surface (Fig. 1) for different values of m and x_0 (ranging from 0.1 to 2.5, corresponding to r_0 in the range 0.5 to 12.5 Å at ~350 mM ionic strength) lie on smooth curves that depend only on the value of $(\partial\phi/\partial x)|_{x_0}$. This fact legitimates the hope of finding a correction to the LPBE which depends only on the electric field at the surface, a value which may be readily estimated for biomolecules from the solution of the LPBE itself.

We notice further that the LPBE potential at the surface is always overestimated with respect to the PBE. In the range examined, the surface LPBE potential may be up to almost 5 times larger than the PBE potential. As expected, for low values of the PBE potential, the LPBE and the PBE give the same result. For large values of the PBE potential at the surface this is determined only by $(\partial\phi/\partial x)|_{x_0}$ (ranging here from −1.0 to −40.0). In particular this may be rationalized by considering that in such cases the electric field is very strong and under its scaling length all geometries resemble the planar geometry, for which the potential is related in a simple fashion to the electric field:

$$\phi_{\mathrm{PBE}} \approx 2 \ln\left(\left|\frac{\partial\phi}{\partial x}\right|_{x_0}\right) \qquad (13)$$

We have chosen the following function which preserves the theoretical asymptotic behavior of the surface potential from the LPBE versus that from the PBE, to fit the curves reported in Fig. 1:

$$\bar{\phi}_{\mathrm{PBE}} = A\left(\frac{\partial\phi}{\partial x}\Big|_{x_0}\right) \cdot \tanh\left(\frac{\phi_{\mathrm{LPBE}}}{A\left(\frac{\partial\phi}{\partial x}\Big|_{x_0}\right)}\right) \qquad (14)$$

where $\bar{\phi}_{\mathrm{PBE}}$ indicates the estimate for the correct (PBE) potential and

$$A\left(\frac{\partial\phi}{\partial x}\Big|_{x_0}\right) \quad (A(u) = -3.037 + 0.1940u + 0.00227u^2)$$

has been built as a quadratic function whose coefficients have been determined from direct fit of the best fit values of

$$A\left(\frac{\partial\phi}{\partial x}\Big|_{x_0}\right)$$

corresponding to different values of $(\partial\phi/\partial x)|_{x_0}$.

The wide range of applicability of the above correction is apparent. Note that in Fig. 1 the value of $\phi_{\mathrm{LPBE}}|_{x_0}$ varies over a very large range and that the value of $(\partial\phi/\partial x)|_{x_0}$ varies from −1.0 to −40.0).

Electrostatic potentials outside the model molecules

We have applied the same correction to the potential using the local values of $\partial\phi/\partial x$ at varying distances from the

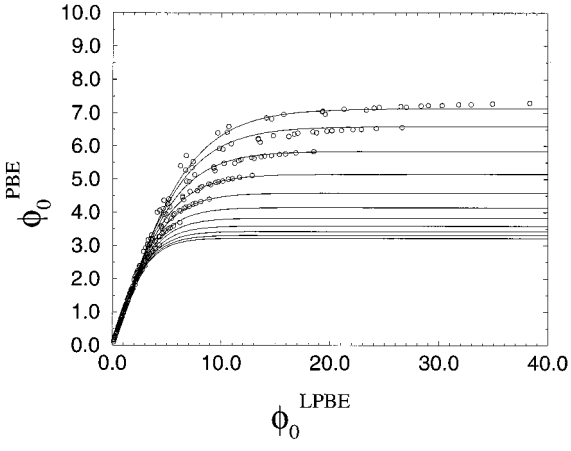

FIGURE 1 $\phi_o = \phi|_{x_0}$ obtained from the PBE versus $\phi_o = \phi|_{x_0}$ obtained from LPBE for various values of the shape parameters m and x_0. The data computed for each value of $(\partial\phi/\phi x)|_{x_0}$ and different values of m and x_0 group along curves which have been described by Eq. 14:

$$\bar{\phi}_{PBE} = A\left(\frac{\partial\phi}{\partial x}\Big|_{x_0}\right) \cdot \tanh\left(\frac{\phi_{\mathrm{LPBE}}}{A\left(\frac{\partial\phi}{\partial x}\Big|_{x_0}\right)}\right)$$

where $\bar{\phi}_{\mathrm{PBE}}$ indicates the estimate for the correct (PBE) potential and the function $A((\partial\phi/\partial x)|_{x_0})$ has the following form: $A(u) = -3.037 + 0.1940u + 0.00227u^2$. The coefficients in the latter equation have been determined by best fit of all points in the plot.

surface (Fig. 2). Although the correction brings the LPBE solution closer to the PBE curve, the two are still too distant for the approximation to be useful away from the surface (at least in a rather extreme case like the one reported in Fig. 2). The main reason for this is that the decay of the LPBE potential is far too slow compared to that of the PBE potential. Obviously, although at the surface the boundary condition is the same for both equations and therefore the derivative of the LPBE potential used for correction is the same as that for the PBE, away from the surface we must use the derivative from the LPBE, which is significantly larger than the derivative from the PBE (Fig. 2). This partly compensates for the slower decay.

Another alternative to obtaining the potential from the LPBE would be to consider an effective potential, as described below, which, substituted in the nonlinearized PBE, reproduces the ionic charge density of the LPBE. The results (shown in Fig. 2 for a highly charged system) are less satisfactory than those obtained with our correcting formula (Eq. 14).

Free energies

The value of the potential at the surface is sufficient to compute the free energy of SSG in the LPBE approach.

Indeed, for the LPBE the only free energy term would be $(\Delta G^{ef}/kT) = (\phi(x_0)/2)$. For the PBE this term would be accurate up to the order of the integral of $(2\phi(x_0)^4/4!)$ over the outer space of the molecule. A comparison of the estimated free energy per unit charge obtained from the LPBE and the PBE is reported in Fig. 3. For values >1 kT (which corresponds to a reduced potential at the surface equal to 2.0) the LPBE overestimates the free energy. Although the term $(\Delta G^{ef}/kT) = (\phi(x_0)/2)$ may constitute the most relevant contribution to the PBE free energy, this is not necessarily close to that estimated via the LPBE. So there

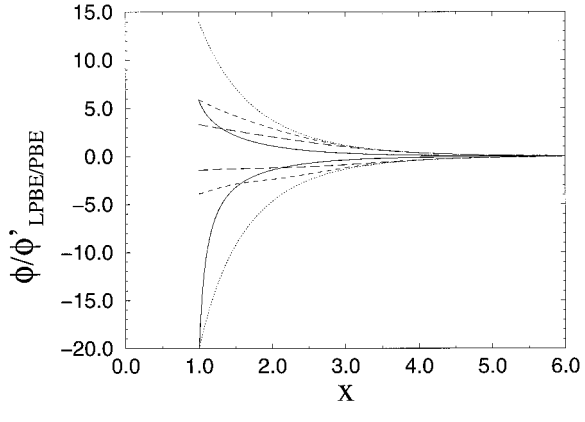

FIGURE 2 ϕ and $\partial\phi/\partial x$ plotted as a function of the reduced distance from the center of a charged cylinder ($m = 1.0$, $x_0 = 0.5$, and $(\partial\phi/\partial x)|_{x_0} = -20.0$) for the PBE (*solid lines*) and LPBE (*dotted lines*). The LPBE potential, corrected according to the local LPBE electric field, is shown (*dashed line*). The plot of the "effective" LPBE potential and of its derivative is also shown (*long dashed lines*).

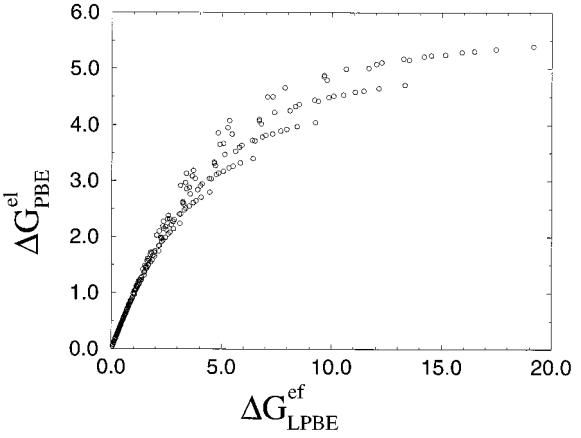

FIGURE 3 $\Delta G^{el}/kT$ from the PBE versus $\Delta G^{ef}/kT$ from the LPBE.

are two main sources of errors in approximating the PBE free energy with the LPBE free energy: consistent overestimation of the potential at the surface and neglect of the contribution to the free energy density integral from the outer space, which is smaller and positive. The two effects partly compensate for each other.

For the studied SSG we have estimated the different contributions to the free energy integral from the surface charges and the outer space to the free energy per unit charge on the surface. It is seen from Fig. 4 that for a global free energy up to 1.0 kT per unit charge on the surface, the free energy from the outer space is negligible. This is also roughly the range of applicability of the LPBE and therefore also the range through which the free energy estimates obtained via the LPBE and the PBE are close.

Even in this range it should be remembered that the LPBE and PBE differ enough to prevent any attempt to substitute the LPBE solution in the equation for the PBE free energy, because even small differences are magnified by the hyperbolic functions. Somewhat better (but still approximate) results are obtained when considering that the mobile charge density in

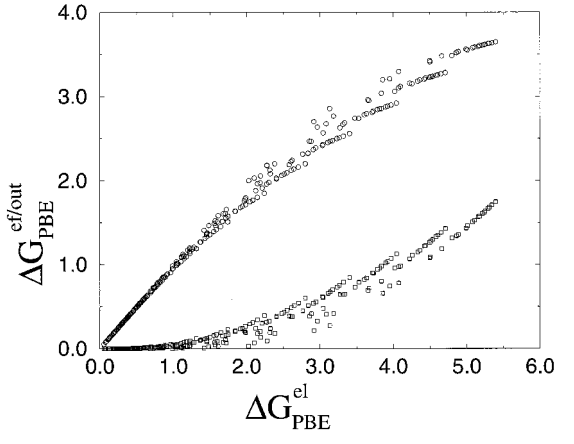

FIGURE 4 $\Delta G^{ef}/kT$ (*circles*) and $\Delta G^{out}/kT$ (*squares*) contribution to the electrostatic free energy versus the electrostatic free energy $\Delta G^{el}/kT$ from the PBE.

the LPBE is given by $\Sigma_i c_i^\infty (z_i^2 q^2 U^{LPBE}/kT)$. We can define an effective potential $\tilde{U}$ such that

$$\sum_i c_i^\infty z_i q \exp\left(-\frac{z_i q \tilde{U}}{kT}\right) = \sum_i c_i^\infty \frac{z_i^2 q^2 U^{LPBE}}{kT} \qquad (15)$$

The behavior of the effective potential for a high surface potential is shown in Fig. 2. For lower potentials this would be closer to the PBE potential. Employing the effective potential in the PBE expressions for the free energy ($\Delta G^{out} = \Delta G^{em} + \Delta G^{mob} + \Delta G^{solv}$) leads to reasonable estimates for the term ΔG^{out} for small values of the free energy (Fig. 5). For high potentials the use of an effective potential brings the term ΔG^{out} into the same range as the corresponding PBE one, although the latter is much smaller. We have also computed the term ΔG^{out} using the corrected LPBE potential and similar considerations apply. For those systems where ΔG^{out} per unit charge on the surface is lower than, say, 0.5 kT, the estimates for ΔG^{out}, obtained via either the effective or the corrected LPBE potential, are not dramatically distant from the PBE values. Although the values of ΔG^{out} span for the studied systems a range of approximately 2.0 kT per unit charge on the surface, in usual biomolecular systems this contribution to the free energy integral will be much lower. Indeed, we have chosen the set of boundary conditions in order to represent also possibly intense local electric fields. Rarely, however, will these conditions apply to the whole surface.

In summary, for the SSG studied it is seen that both the potentials and the free energies estimated using the LPBE are accurate up to values of the electrostatic potential at the surface of $2(kT/q)$. A simple electric field-dependent correction at the surface reproduces with high accuracy the PBE electrostatic potential at the surface. The free energy estimates obtained via the LPBE, taking into account the contribution to the free energy integral from the outer space in a reasonable fashion, are accurate up to few tenths of kT per unit charge, up to reduced surface potentials of 2 to 3.

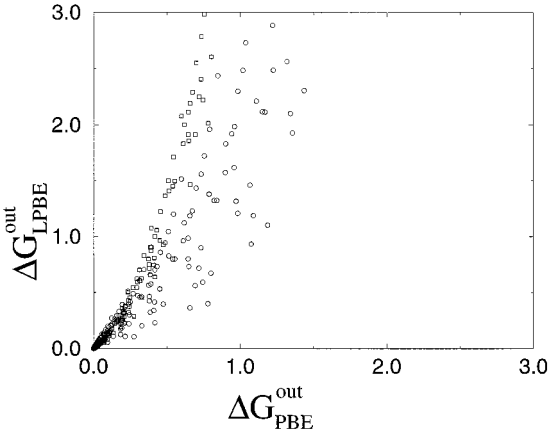

FIGURE 5 $\Delta G^{out}/kT$ from the LPBE using the correcting formula (Eq. 14) (*squares*) or estimated through an effective potential (Eq. 15) from the LPBE (*circles*) versus $\Delta G^{out}/kT$ obtained from the PBE. Only values in the range 0.0 to 3.0 for both variables are shown.

Biomolecular systems

Next we discuss the limits of applicability of the LPBE for a few systems of biological interest that may be representative of a diversity of shapes and that correspond to high charge densities. For low-charge systems the LPBE is usually in striking agreement with the PBE.

As for the SSG we discuss separately three areas where we can extend and put to use the results obtained for the SSG models: first, calculation of the electrostatic potential at the surface of the molecule; second, calculation of the electrostatic potential outside the molecule; and third, calculation of the free energies of the system. In addition we discuss the correction of the electrostatic potential inside the molecule.

Most of the results are illustrated for the homeodomain-DNA complex (Fig. 6), the most irregular of the systems studied in terms of shape and charge density. Results for the other systems are summarized in few figures and in one table. Physiological (145 mM) and low (14.5 mM) ionic strengths have been considered. The agreement between the LPBE and PBE increases with increasing ionic strength (i.e., with better screening of the potential).

Surface electrostatic potentials

Discrepancies between the LPBE and the PBE at the solvent accessible surface for highly charged systems are usually as large as several kT/q at low ionic strengths, as can be seen from Fig. 1. In the studied cases the error from linearization is larger where the potential is larger, as expected, because this is exactly the condition in which the LPBE and the PBE differ. However, note that the linearized equation also does not reproduce in general the PBE potential in those regions where the linearization can be safely applied. This point will be discussed in the next section.

We have applied the correction formula (Eq. 14) at the surface of the biomolecule. The accessibility map was first obtained using the UHBD program and then the boundary points on the grid between the low dielectric cavity and the solvent were selected. For these points the electric field was obtained using finite differences between the potentials in the neighboring points. Finally the reduced electric field was employed in the correction formula. Unlike the SSG considered above, the electric field determined in this way for the LPBE is not the same as for the PBE, but must be considered an estimate of the true electric field. The intensity of the electric field as obtained from the LPBE and PBE for the Antp HD-DNA complex are reported in Fig. 7. The two give almost identical patterns at the surface of the molecules but are different in the surrounding volume, although similar trends are found. This is remarkable be-

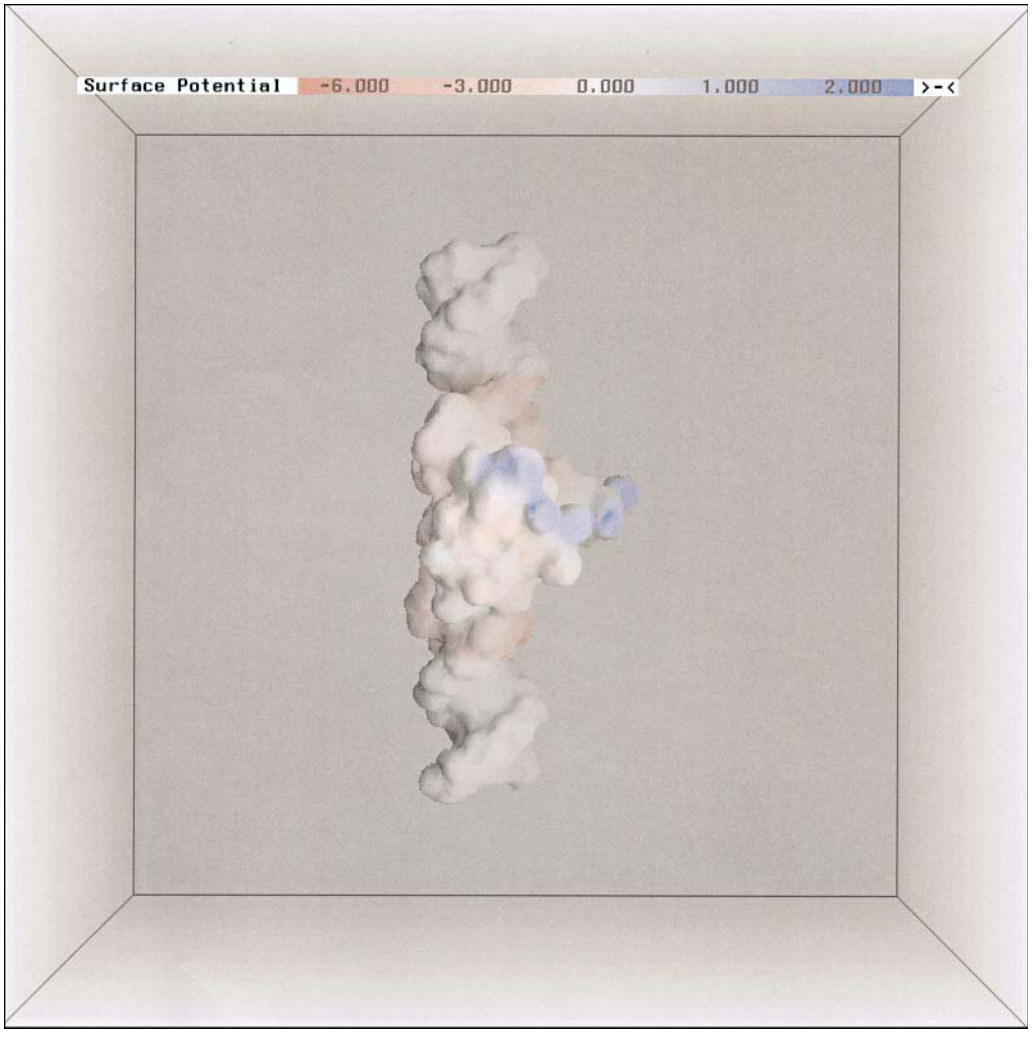

FIGURE 6 The electrostatic potential (in *kcal*/*q* · *mol* units) at the surface of the Antp C39S HD-DNA complex at 14.5 mM ionic strength as obtained from the PBE, visualized with the software GRASP (Nicholls, 1993). A similar, but reduced in magnitude, potential pattern is obtained at 145 mM ionic strength. Only the potential from the last focused region is shown.

cause electrostatic forces in molecular dynamics simulations are computed from the electric field at the surface and inside the molecule, rather than from the potential (Gilson et al., 1993). We found a larger electric field from the LPBE than from the PBE, which is expected to result in a correction slightly larger than that obtained from knowledge of the exact electric field.

The plot of the LPBE electrostatic potential (with and without correction) versus the PBE electrostatic potential at 14.5 mM ionic strength is reported in Fig. 8. It is seen that the correction largely reduces the error in all cases. The distributions of the number of points with the error magnitude at the surface and their integrals are very similar to those obtained in the whole volume surrounding the molecule; therefore, they will not be discussed here.

Results obtained for the same systems at 145 mM ionic strength are very similar, although the range of the potential is reduced by approximately one-fourth.

Electrostatic potentials inside the molecule

The electrostatic potential inside the molecule ($\phi = (qU/kT)$) may be written as the sum of a direct Coulombic term (ϕ_C) due to all atomic partial charges inside the molecule and a reaction field term (ϕ_R) due to polarization charges at interface and ionic charges outside the molecule: $\phi = \phi_C + \phi_R$.

The reaction field inside the molecule satisfies Laplace's equation and therefore can be expanded in any suitable set of basis functions that satisfy Laplace's equation. The coefficients of the expansion are unambiguously determined by the boundary conditions, obtained by subtracting from the electrostatic potential at the surface the easily computed direct Coulombic contribution. Therefore, possessing an accurate description of the potential at the surface allows for an accurate evaluation of the electrostatic potential inside the molecule. To test this point, we have considered the fully protonated form of β-lactoglobulin, which is globular

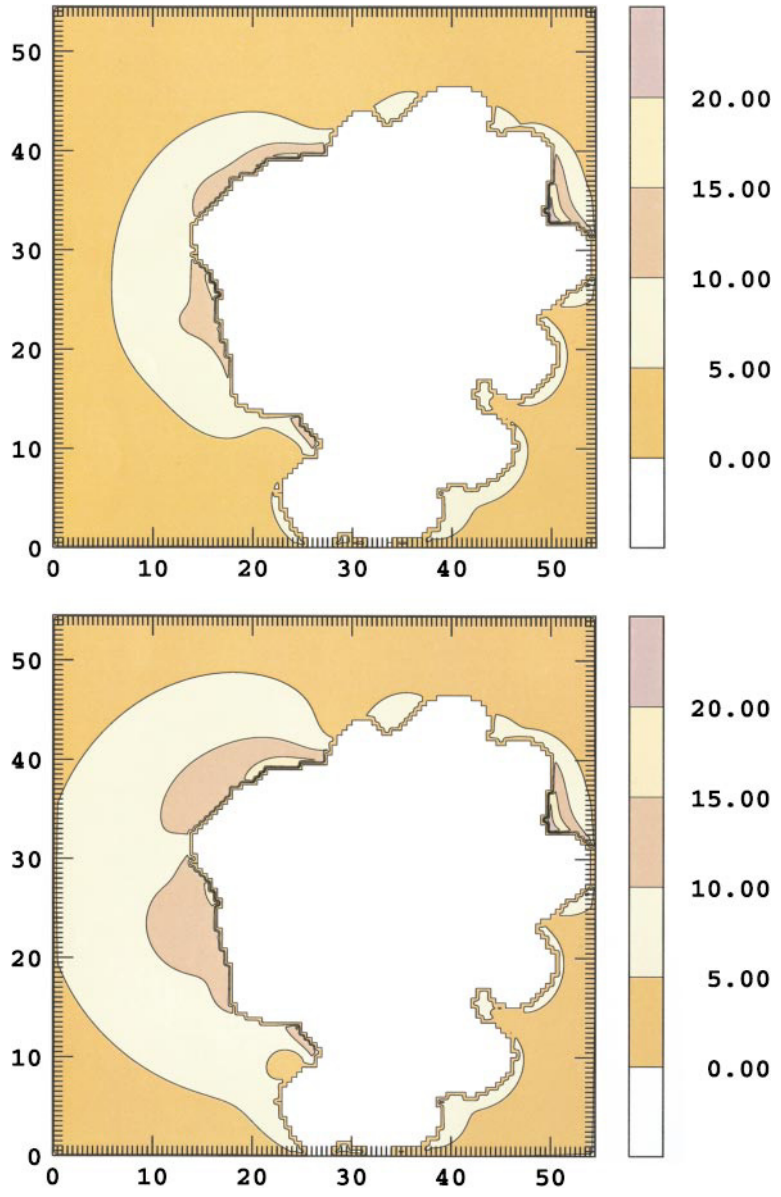

FIGURE 7 The electrostatic field (in reduced $(kT/q)k_D$ units) from the PBE (*upper panel*) and from the LPBE (*lower panel*) in a plane orthogonal to the DNA axis going through the center of geometry of the Antp C39S HD-DNA complex.

overall with a rough surface, and we expanded the reaction field inside the molecule at 15 mM ionic strength using the following set of functions related to spherical harmonics:

$$\phi_R = \sum_{\substack{l=0,L \\ m=-l,l}} a_{lm} r^l P_{lm}(\cos\vartheta) \begin{Bmatrix} \sin(m\varphi) \\ \cos(m\varphi) \end{Bmatrix} \qquad (16)$$

where $P_{lm}(\cos\vartheta)$ are Legendre's polynomials and r, ϑ and φ are spherical coordinates (Jackson, 1962) and $L = 10$ in all calculations.

The expansion coefficients $\{a_{lm}\}$ are obtained by best fit of the boundary conditions. This procedure amounts to solving a set of linear equations via Singular Value Decomposition retaining all eigenvalues (see Press et al., 1990). For other molecular shapes, other basis functions or other ways to solve Laplace's equation should be chosen. Virtually identical reaction field potentials at atomic positions (RMSD = 0.045 ($kcal/q \cdot mol$)) were obtained using boundary conditions derived from PBE and corrected LPBE, clearly distinguishable from the case in which boundary conditions from LPBE had been employed (RMSD = 0.490 ($kcal/q \cdot mol$)).

Electrostatic potentials outside the molecule

An error similar to that found at the surface of the biomolecules studied is found in the whole space surrounding the molecules. As for SSG, the LPBE consistently overestimates the potential. A simple explanation is that because the PBE, due to the hyperbolic function, puts more counterions in the proximity of the molecule, the potential decays faster. The correction determined at the surface of SSG also retains its validity (although to a lesser extent) away from the surface.

The maps reported in Fig. 9 show, for instance, that the range of the error in absolute value on the potential in a

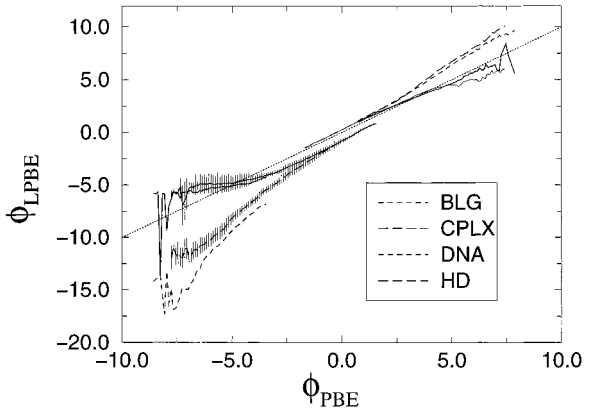

FIGURE 8 The average electrostatic potential (in kT/q units) from the LPBE (*dashed lines*) and from the corrected (Eq. 14) LPBE (*solid lines*) at the surface of the Antp C39S HD-DNA complex, the isolated DNA and HD and fully protonated β-lactoglobulin at 14.5 mM ionic strength versus the electrostatic potential obtained from the PBE. CPLX, HD, DNA and BLG stand for the homeodomain-DNA complex, the isolated homeodomain, the isolated DNA stretch and fully protonated β-lactoglobulin. The RMSD are also given as vertical bars only for the Antp C39S HD-DNA complex to avoid excessive plot crowding. The corrected and uncorrected LPBE can be easily paired because they obviously span the same range of the x-axis.

plane orthogonal to the DNA longitudinal axis going through the center of geometry of the Antp C39S HD-DNA complex can be as large as $3(kT/q)$. It is apparent that the error is larger where the potential is larger, although the difference is not as large as the difference between the potential and the hyperbolic sine of the potential. The error is halved by the correction.

The results shown in Fig. 9 are typical, although the range of the error varies depending on the system and the ionic concentration. A useful representation of the results, in order to visualize the information contained in almost one million points, is the distribution of points corresponding to small intervals on the error axis and its integral. This is a measure of the reliability of the linearization approximation.

For instance, the quantitative analysis for the Antp C39S homeodomain-DNA complex (Fig. 10) at 14.5 mM ionic strength shows that the distribution of the error for the corrected LPBE has a sharp peak centered at $\sim 0.8(kT/q)$, whereas the error for the uncorrected LPBE follows a smooth distribution curve.

The cumulative distribution of the error is also interesting and places 99% of the points for the corrected LPBE within $1(kT/q)$ of the PBE ones, although for the uncorrected LPBE a significant amount of points (more than 1%) is affected by an error larger than $3(kT/q)$.

These are typical results at low ionic strengths. The LPBE at larger ionic strengths performs better for globular systems. This is a simple consequence of the overall decrease in magnitude of the potential due to more efficient ionic screening and reduced polyelectrolytic effects. However, in this case the correction also brings the values of the potential closer to those obtained by the PBE.

Sometimes the LPBE or the spherical Debye-Hückel potential is used to compute electrostatic fields far from the molecule. A problem not always recognized with this usage of the LPBE is that the validity of the linearization condition ($(z_i qU/kT) \ll 1$) in a certain region of space does not guarantee that the solution of the LPBE and PBE will coincide, because the boundary conditions in that region might be influenced by the solution of the equation in regions of the space where the linearization condition is not valid. This is particularly clear, for instance, from the plot of the potential versus the distance from the axis of a cylinder reported in Fig. 2. The plot of the LPBE potential in the space surrounding the homeodomain-DNA complex versus the PBE potential is very similar to that obtained at the surface and confirms this point even for very small values of the PBE potential.

Electrostatic free energies

A word is due on electrostatic free energies with finite difference solution of the PBE equation. Whereas the contributions to the free energy integral from the outer space of the molecule may be obtained analogously to the SSG, for biomolecules with discrete charge distributions, there is not a direct counterpart to the free energy contribution due to the surface charge term. Indeed the term ΔG^{ef} is strongly dependent on the discretization of the charge and one is usually interested in computing physical quantities, like the reaction field energy, obtained through subtraction of self-energy, grid-dependent terms. The reaction field, i.e., the field due to salt and solvent polarization charges, may be obtained alternatively solving the Poisson equation with standard methods within the molecule with Dirichlet boundary conditions obtained via a finite difference PBE or LPBE calculation. The degree of accuracy of the solution of the Poisson equation will ultimately depend on the accuracy of the boundary conditions. We tested this point on the fully protonated form of β-lactoglobulin. The correction on ΔG^{ef}, computed from the solution of Laplace's equation inside the molecule, as described above), is -5.7 kcal/mol both for the corrected LPBE and PBE. This figure is slightly different from -6.4 kcal/mol obtained from the UHBD program, as a possible consequence of the poor choice for the set of basis functions (or Laplace's equation solver) or the slightly different definition of the boundary in our model and the more accurate definition given by UHBD.

The contributions to the free energy density integral from regions outside the molecule depend on the potential through hyperbolic functions; therefore, small errors in the potential will be greatly amplified. The conclusions reached on SSG also apply here, though the discrepancy is less severe, ranging up to one or two orders of magnitude. Using the effective potential defined above (Eq. 15) is a simple way to offset the exponential terms. Indeed, the figures obtained for ΔG^{out} are in the correct range but consistently underestimated. Similar quantitative results on all terms are obtained using the corrected LPBE potential, which also

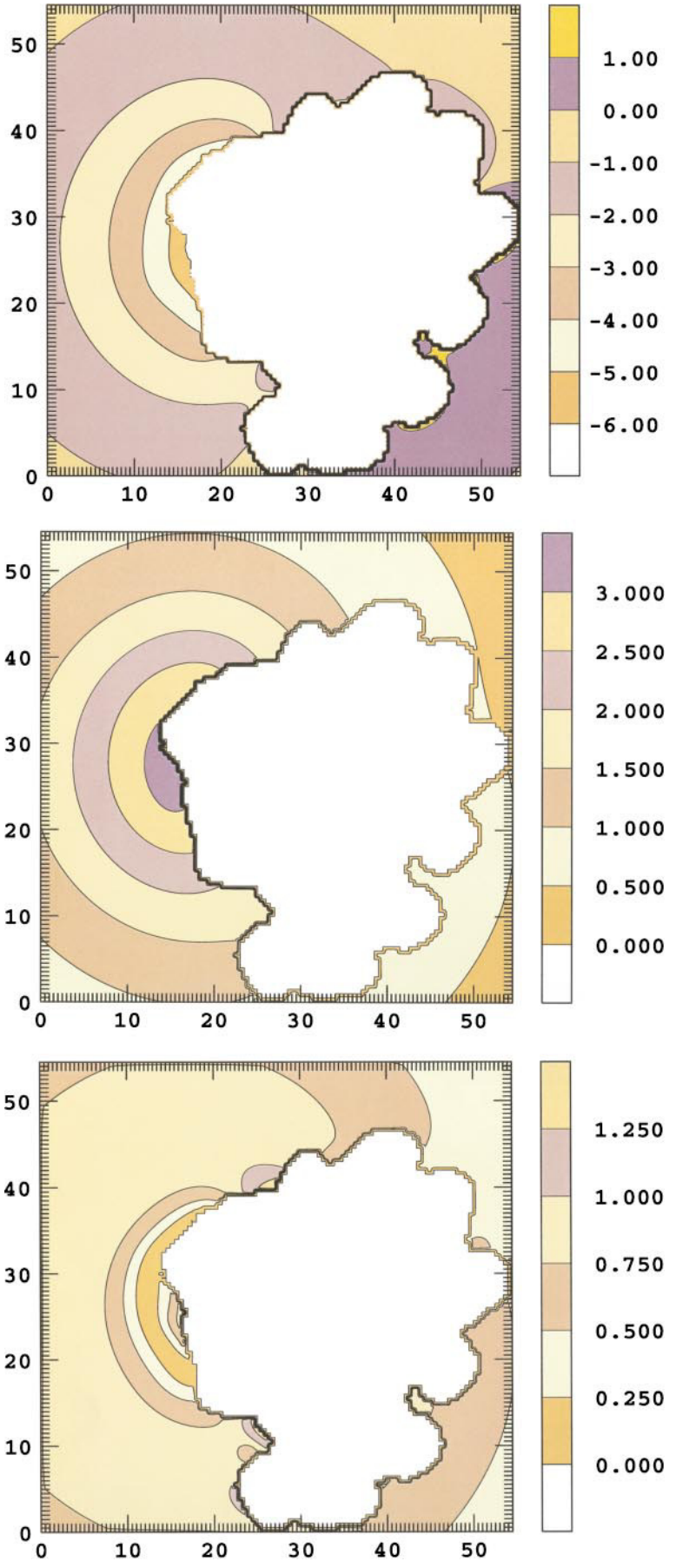

FIGURE 9 Maps of the electrostatic potential (in kT/q units) from the PBE (*upper panel*) in a plane orthogonal to the DNA axis going through the center of geometry of the Antp C39S HD-DNA complex at 14.5 mM ionic strength. The difference in absolute value between the potential obtained from the LPBE (*middle panel*) and the corrected (Eq. 14) LPBE (*lower panel*) are shown.

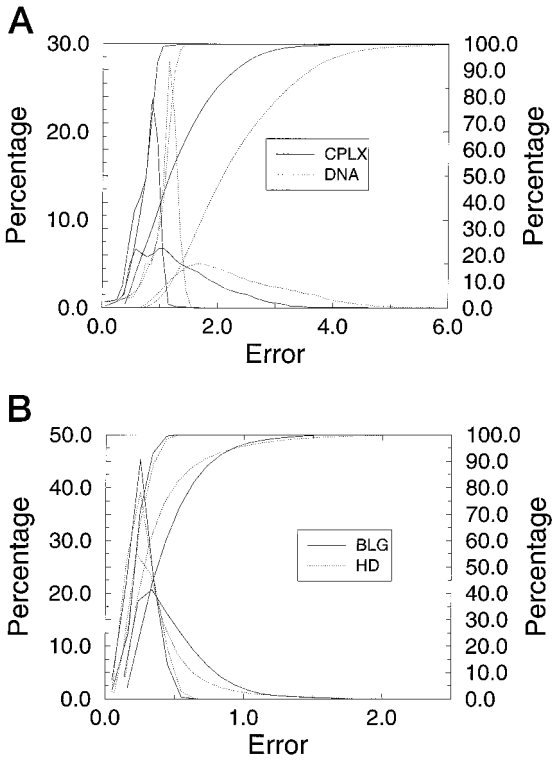

FIGURE 10 The distribution of the difference (in kT/q units) in absolute value between the PBE potential and the potential obtained from the LPBE and the corrected (Eq. 14) LPBE for the Antp C39S HD-DNA complex and isolated DNA (*upper panel*), and isolated homeodomain and fully protonated β-lactoglobulin (*lower panel*) at 14.5 mM ionic strength, shown as percentage of points in small intervals of the x-axis. The integral of the distribution is also shown. The uncorrected LPBE curves are recognizable because they span a larger error range.

brings the obtained figures in the correct range, but seems to consistently overestimate the free energy. It seems that the average of the two is able to reproduce the PBE ΔG^{out}.

From Table 1 the different behavior of the LPBE equation in low and relatively high ionic strengths is apparent. In the latter case the electrostatic potential becomes smaller; in most of the space it is within the range of one or two kT/q. Contributions to the free energy density integral are, to a first approximation, proportional to the integral of $(2\phi(x_0)^4/4!)$. If this term is small, then it is also legitimate to expect that the linearization condition holds. This is true for overall globular protein like the homeodomain or β-lactoglobulin at 145 mM, while it is seen that the polyelectrolytic behavior of the DNA, partly neutralized by the homeodomain in the complex, leads, as expected, to high potentials and therefore to large discrepancies between the PBE and LPBE potentials. As a consequence the free energy is not properly recovered from the LPBE potential.

CONCLUSIONS

The LPBE is a widely used approximation of the PBE for biomolecular simulations. Results on SSG show that the potential at the surface obtained using the LPBE may be easily corrected to reproduce fairly accurately that obtained from the PBE. The correction depends on the reduced electric field at the surface, but does not involve any geometrical parameter. Although it might be surprising that systems as different as spheres, cylinders, and planes behave very similarly in this respect, the results may be rationalized taking into account that the deviations from the linearization condition depend on the ratio between the

TABLE 1 Contributions to the electrostatic free energy

	at 14.5 mM ionic strength															
	CPLX				DNA				HD				BLG			
	PBE	LPBE*	LPBE$^{\#}$	LPBE§	PBE	LPBE*	LPBE$^{\#}$	LPBE§	PBE	LPBE*	LPBE$^{\#}$	LPBE§	PBE	LPBE*	LPBE$^{\#}$	LPBE§
ΔG^{em}	−13.3	−4.1	−24.3	−14.2	−26.8	−8.0	−63.7	−35.9	−5.2	−1.8	−6.1	−3.9	−6.7	−2.3	−8.1	−5.2
ΔG^{mob}	26.5	8.2	48.7	28.4	53.6	16.0	127.4	71.7	10.5	3.5	12.1	7.8	13.3	4.5	16.1	10.3
ΔG^{solv}	−6.6	−3.0	−12.4	−7.7	−12.6	−5.6	−29.3	−17.5	−3.0	−1.4	−3.7	−2.6	−4.0	−1.8	−5.0	−3.4
ΔG^{out}	6.6	1.1	12.0	6.5	14.2	2.4	34.4	18.4	2.3	0.3	2.3	1.3	2.6	0.4	3.0	1.7
	at 145 mM ionic strength															
	CPLX				DNA				HD				BLG			
	PBE	LPBE*	LPBE$^{\#}$	LPBE§	PBE	LPBE*	LPBE$^{\#}$	LPBE§	PBE	LPBE*	LPBE$^{\#}$	LPBE§	PBE	LPBE*	LPBE$^{\#}$	LPBE§
ΔG^{em}	−9.2	−6.2	−13.5	−9.8	−16.7	−11.2	−27.5	19.4	−4.6	−3.0	−5.7	−4.3	−5.7	−3.9	−6.9	−5.4
ΔG^{mob}	18.4	12.3	27.0	19.6	33.3	22.4	55.0	38.7	9.1	6.0	11.4	8.7	11.3	7.8	13.8	10.8
ΔG^{solv}	−6.6	−5.2	−9.7	7.4	−11.4	−9.2	−18.9	−14.1	−3.4	−2.6	−4.3	−3.4	−4.4	−3.5	−5.5	−4.5
ΔG^{out}	2.6	0.9	3.8	2.4	5.2	2.0	8.6	5.3	1.1	0.4	1.4	0.9	1.2	0.4	1.4	0.9

The contributions to the free energy density integral from the outer space of the biomolecules (see Eqs. 8–12). CPLX, HD, DNA, and BLG stand for the homeodomain-DNA complex, the isolated homeodomain, the isolated DNA stretch and fully protonated β-lactoglobulin, respectively. In the column labeled PBE the values obtained with the full PBE are reported. In the column labeled LPBE* the effective potential (Eq. 15) is employed. In the column labeled LPBE$^{\#}$ the corrected LPBE potential (Eq. 14) is employed. In the column LPBE§ the mean between LPBE* and LPBE$^{\#}$ is reported.

*Effective potential from Eq. 15 used to compute the free energy.

$^{\#}$Corrected LPBE potential from Eq. 14 used to compute the free energy.

§Mean between the previous two columns.

electric field and the Debye scale length and not on geometrical parameters.

Results on high charge density systems show that there are limitations to the applicability of the LPBE to biomolecular systems at low ionic strength (14.5 mM) and to a lesser extent at higher ionic strength (145 mM). For systems in physiological ionic strength with lower charge density the LPBE gives virtually the same results as the PBE. The range of the error in the potential for the LPBE (compared to the PBE) spans few kT/q for the systems studied here. The LPBE can be corrected with a simple formula that does not involve any geometrical parameter, as inferred from the study of SSG. The correction allows for more accurate calculation of the electrostatic free energy of the systems.

APPENDIX A

The PBE for systems with a simple geometry

The PBE in the solution surrounding SSG is written in the following form:

$$\tilde{\nabla}\cdot\tilde{\nabla}U = -\frac{4\pi}{\epsilon}\sum_{\mathrm{i}} c_{\mathrm{i}}^{\infty} z_{\mathrm{i}} q \exp\left(\frac{-z_{\mathrm{i}} qU}{kT}\right) \tag{A1}$$

with the boundary conditions given by the field at the low dielectric region surface.

Particularly when uniformly charged planes, cylinders, or spheres are considered, the solution depends on a single variable and the equation may therefore be recast as:

$$\frac{\partial^2 U}{\partial r^2} + \frac{m}{r}\frac{\partial U}{\partial r} = -\frac{4\pi}{\epsilon}\sum_{\mathrm{i}} c_{\mathrm{i}}^{\infty} z_{\mathrm{i}} q \exp\left(\frac{-z_{\mathrm{i}} qU}{kT}\right) \tag{A2}$$

where m is 0, 1, and 2 for the plane, cylinder, and sphere respectively, and r is the distance from the surface of the plane, from the axis of the cylinder, or from the center of the sphere for the corresponding values of m. The boundary condition is given by the value of $\partial U/\partial r$ at r_0 which defines the boundary (i.e. the radius of the sphere or the cylinder, and any arbitrary position of the planar boundary). With the aid of the reduced potential $\phi = (qU/kT)$ and reduced length $x = k_{\mathrm{D}} r$, where $k_{\mathrm{D}} = \sqrt{4\pi\Sigma_{\mathrm{i}} c_{\mathrm{i}}^{\infty} z_{\mathrm{i}}^2 q^2/\epsilon kT}$ is the Debye screening constant, for a 1:1 electrolytic solution, the PBE may be rewritten as:

$$\frac{\partial^2 \phi}{\partial x^2} + \frac{m}{x}\frac{\partial \phi}{\partial x} = \sinh(\phi) \tag{A3}$$

The solution of the equation is determined by the boundary condition $\phi'(x_0)$.

In order to have reasonable values for both x_0 and $\phi'(x_0)$ we considered the following surface area elements in terms of the Bjerrum length $l_{\mathrm{B}} = (q^2/\epsilon kT)$:

$$S = l_{\mathrm{B}}^2 \times \pi \quad \text{for the plane,}$$

$$S = l_{\mathrm{B}} \times 2\pi r_0 \quad \text{for the cylinder, and}$$

$$S = 4\pi {r_0}^2 \quad \text{for the sphere,}$$

or with the previous notation:

$$S = l_{\mathrm{B}}^{(2-\mathrm{m})} \times 2^{\mathrm{m}} \pi {r_0}^{\mathrm{m}} \tag{A4}$$

Notice that for a given $\phi'(x_0)$ the number of charges z in the area S is:

$$z = \frac{-k_{\mathrm{D}} l_{\mathrm{B}}}{4}\phi'(x_0) \quad \text{for the plane}$$

$$z = \frac{-x_0}{2}\phi'(x_0) \quad \text{for the cylinder}$$

$$z = \frac{-x_0^2}{k_{\mathrm{D}} l_{\mathrm{B}}}\phi'(x_0) \quad \text{for the sphere}$$

or in a general form:

$$z = \frac{-x_0^{\mathrm{m}}}{2^{2-\mathrm{m}}(k_{\mathrm{D}} l_{\mathrm{B}})^{\mathrm{m}-1}}\phi'(x_0) \tag{A5}$$

Usual biomolecular systems modeled as uniformly charged planes, cylinders, or spheres typically have average charge densities lower than two charges per element area $S = l_{\mathrm{B}}^2 \times \pi$. Because the product $k_{\mathrm{D}} l_{\mathrm{B}}$ will range for typical monovalent ionic solutions between 0.2 and 2 (corresponding to ionic strengths in the 7–700 mM range), reasonable values of $\phi'(x_0)$ will be <40.

The free energy per unit charge (expressed in kT units) may be easily calculated:

$$\frac{\Delta G^{\mathrm{ef}}}{kT} = \frac{\phi(x_0)}{2} \tag{A6}$$

$$\frac{\Delta G^{\mathrm{em}}}{kT} = -\frac{1}{z}\int_{\mathrm{V}} \frac{k_{\mathrm{D}}^2}{8\pi l_{\mathrm{B}}}\phi \sinh(\phi)\mathrm{d}V \tag{A7}$$

$$\frac{\Delta G^{\mathrm{mob}}}{kT} = \frac{2}{z}\int_{\mathrm{V}} \frac{k_{\mathrm{D}}^2}{8\pi l_{\mathrm{B}}}\phi \sinh(\phi)\mathrm{d}V \tag{A8}$$

$$\frac{\Delta G^{\mathrm{solv}}}{kT} = -\frac{2}{z}\int_{\mathrm{V}} \frac{k_{\mathrm{D}}^2}{8\pi l_{\mathrm{B}}}(\cosh(\phi) - 1)\mathrm{d}V \tag{A9}$$

The scaled volume element $(k_{\mathrm{D}}^2/z8\pi l_{\mathrm{B}})\mathrm{d}V$ is written as: $(k_{\mathrm{D}} l_{\mathrm{B}}/8z)\mathrm{d}x$, $(x/4z)\mathrm{d}x$ and $(x^2/2l_{\mathrm{B}}k_{\mathrm{D}}z)\mathrm{d}x$ for the plane, cylinder, and sphere, respectively or, substituting the expression for the charge z, in general form:

$$\frac{k_{\mathrm{D}}^2}{z8\pi l_{\mathrm{B}}}\mathrm{d}V = -\frac{1}{2\phi'(x_0)}\left(\frac{x}{x_0}\right)^{\mathrm{m}}\mathrm{d}x \tag{A10}$$

Therefore also the free energy stabilization per unit charge is dependent only on the reduced variables x_0 and $\phi'(x_0)$.

APPENDIX B

Previous results on systems with a simple geometry and relevant length scales

The limits of applicability of the LPBE on SSG have been known for some time and empirical formulae have been put forward to recover from the LPBE potential, the PBE potential, or also the PBE charging free energy (see below). Some of the previous results unify the treatment for different shapes and it is therefore tempting to try to further generalize these results to shape-independent formulae.

We aim to find a general relationship between the solution of the LPBE and that of the PBE that avoids the definition of any geometrical parameter, because this would not be unambiguously identified for irregularly shaped

biomolecules. (However, for a definition of a radius of curvature in conjunction with protein electrostatics, see Abagyan and Totrov (1994).)

We review hereafter some important general results obtained by Stigter (1975, 1978) and the group of Gueron and Weisbuch (1979, 1980; Weisbuch and Gueron, 1981, 1983; Gueron and Demaret, 1992).

In particular, Stigter (1975, 1978, and references cited therein) furnished a table of correction factors for some thermodynamic quantities derived from the LPBE for cylinders and spheres and made the following observations:

(1) for high charge densities the counterion concentration at the surface is rather insensitive to salt dilution;
(2) for spheres and cylinders possessing the same charge density and the same radius of curvature ($R_C = r_0$ for the sphere and $R_C = 2r_0$ for the cylinder), in similar ionic conditions, the surface potential is similar; and
(3) for high charge densities spheres, cylinders, and planes have similar surface potentials.

Gueron and Weisbuch (1980) extend these observations and recognize the importance of the interplay of two natural scale lengths of the problem. They compare spheres and cylinders characterized by the same parameter $\eta = (r_0/\lambda_D$ (where $\lambda_D = (1/k_D)$, the inverse of the Debye screening constant, is the Debye length), same surface charge density σ and related parameter $\xi = \pi(\sigma/q)l_B R_C$.

The invariance of the surface concentration of counterions (CIV = Concentration in the Immediate Vicinity) with ionic strength is also observed here. Most important, Gueron and Weisbuch (1980) observe that the CIV is determined mainly by the surface charge density (for ionic concentrations larger than 10 mM) and not by the shape. In later works they propose some approximate expressions for the potential and the free energy for spheres and cylinders in reference to a plane possessing the same surface charge density (Gueron and Weisbuch, 1979, 1980; Weisbuch and Gueron, 1981; Gueron and Demaret, 1992). In order to classify SSG Weisbuch and Gueron (1983) propose to consider an additional scale length which is set by the electric field (i.e., for SSG, by the surface charge density).

This scale length is defined as:

$$l_e = \frac{\left(\frac{\partial \phi}{\partial r}\right)_{r=r_0}}{\left(\frac{\partial^2 \phi}{\partial r^2}\right)_{r=r_0}} \tag{B1}$$

For the plane this can be written as:

$$l_e = \frac{\lambda_D}{\cosh\left(\frac{\phi(r_0)}{2}\right)} \tag{B2}$$

Then a related quantity Θ may be defined as the ionic layer thickness:

$$\Theta = \frac{1}{2\pi\left(\frac{\sigma}{q}\right)l_B} \tag{B3}$$

for the plane this is the distance from the surface at which ionic concentration is reduced to one-quarter of that at the surface, when $\phi(x_0) \gg 1$.

By using the first integration of the PBE for the plane we obtain:

$$\left(\frac{\partial \phi}{\partial r}\right)_{r=r_0} = \frac{2\sinh\left(\frac{\phi(r_0)}{2}\right)}{\lambda_D} = \frac{2}{\Theta} \tag{B4}$$

which may be further rearranged:

$$\frac{\lambda_D}{\Theta} = \sinh\left(\frac{\phi(r_0)}{2}\right) \tag{B5}$$

The latter equation clearly shows that the linear or nonlinear regime depends upon the ratio λ_D/Θ, i.e., following from Eq. B4, the reduced electric field at the surface.

When Eq. B5 is substituted in Eq. B2 the electric field scale length is expressed in terms of

$$l_e = \frac{\lambda_D}{\left(1 + \frac{\lambda_D^2}{\Theta^2}\right)^{1/2}} \tag{B6}$$

The latter relation shows that the relevant scale length for the electric field is either λ_D or Θ depending upon their ratio.

The previous discussion has been summarized for cylindrical geometries in the following table by Rouzina and Bloomfield (1996), in which the mutual relationship between the three scale lengths mentioned and the behavior of the PBE solution are compared:

$$\lambda_D < \Theta < R_C \quad \text{linear, planar}$$

$$\Theta < \lambda_D < R_C \quad \text{nonlinear, planar}$$

$$\Theta < R_C < \lambda_D \quad \text{nonlinear, cylindrical}$$

$$\lambda_D < R_C < \Theta \quad \text{linear, cylindrical (pseudoplanar)}$$

$$R_C < \lambda_D < \Theta \quad \text{linear, cylindrical}$$

$$R_C < \Theta < \lambda_D \quad \text{weakly nonlinear, cylindrical}$$

An interesting observation of that study was that for a highly charged cylinder the ionic distributions, properly scaled, are very similar to those of a plane of the same charge density. Since the charge density is directly related to the electric field, the distance from the surface was also scaled by λ_D, and the comparison was made for equal ionic strengths, we may recast that observation in the following form: planes and cylinders for which the boundary condition $(\partial\phi/\partial x)|_{x_0}$ is fixed show similar behavior.

We further note that of the three relevant scale lengths, λ_D and Θ are also easy to identify for irregularly shaped and charged biomolecules. For these cases the electric field is not given, but may be obtained by solving the PBE, or rather estimated from the solution of the LPBE. Starting from Eqs. B4 and B5 we have identified the reduced electric field at the surface $(\partial\phi/\partial x)|_{x_0}$ as a key parameter to correct the LPBE potential.

We thank Prof. M. Giorgi and Prof. G. Pastore (University of Trieste) for reading and making useful comments on the degree thesis of P. Z., which contained much of the work presented here. We warmly thank P. J. Turner for making the 2D plotting software XMGR available, Albrecht Preusser and the Fritz-Haber-Institut der MPG, Berlin for making the 3D contouring program Xfarbe available, and Anthony Nicholls for making the molecular graphics software GRASP available.

REFERENCES

Abagyan, R., and M. Totrov. 1994. Biased probability Monte Carlo conformational searches and electrostatic calculations for peptides and proteins. *J. Mol. Biol.* 235:983–1002.

Alfrey, T., Jr., P. W. Berg, and H. Morawetz. 1951. The counterion distribution in solutions of rod-shaped polyelectrolytes. *J. Polymer Sci.* 7:543–547.

Antosiewicz, J., J. A. McCammon, and M. K. Gilson. 1994. Prediction of pH-dependent properties of proteins. *J. Mol. Biol.* 238:415–436.

Baginski, M., F. Fogolari, and J. M. Briggs. 1997. Electrostatic and non electrostatics effects on anthracycline DNA binding. *J. Mol. Biol.* 274: 253–267.

Billeter, M., Y. Q. Qian, G. Otting, M. Müller, W. J. Gehring, and K. Wüthrich. 1993. Determination of the nuclear magnetic resonance solution structure of an *Antennapedia*-DNA complex. *J. Mol. Biol.* 234: 1084–1097.

Brooks, B. R., R. E. Bruccoleri, B. D. Olafson, D. J. States, S. Swaminathan, and M. Karplus. 1983. CHARMM: a program for macromolecular energy, minimization, and dynamics calculations. *J. Comput. Chem.* 4:187–217.

Brownlow, S., J. H. Morais Cabral, R. Cooper, D. R. Flower, S. J. Yewdall, I. Polikarpov, A. C. T. North, and L. Sawyer. 1996. Bovine β-lactoglobulin at 1.8 Å resolution: still an enigmatic lipocalin. *Structure.* 5:481–495.

Chapman, D. L. 1913. A contribution to the theory of electrocapillarity. *Phil. Mag.* 25:475–481.

Davis, M. E., and J. A. McCammon. 1990. Electrostatics in biomolecular structure and dynamics. *Chem. Rev.* 90:509–521912.

Davis, M. E., J. D. Madura, J. Sines, B. A. Luty, S. Allison, and J. A. McCammon. 1991. Diffusion-controlled enzymatic reactions. *Methods Enzym.* 202:473–497.

Derjaguin, B., and L. Landau. 1941. A theory of the stability of strongly charged lyophobic sols and the coalescence of strongly charged particles in electrolytic solution. *Acta Phys.-Chim. USSR.* 14:633–662.

Debye, P., and E. Hückel. 1923. Zur theorie der elektrolyte. *Physik. Zeitschr.* 24:185–206.

Fixman, M. 1979. The Poisson-Boltzmann equation and its application to polyelectrolytes. *J. Chem. Phys.* 70:4995–5005.

Fogolari, F., and J. M. Briggs. 1997. On the variational approach to the Poisson-Boltzmann free energies. *Chem. Phys. Lett.* 281:135–139.

Fogolari, F., A. H. Elcock, G. Esposito, P. Viglino, J. M. Briggs, and J. A. McCammon. 1997. Electrostatic effects in homeodomain-DNA interaction. *J. Mol. Biol.* 267:368–381.

Fogolari, F., G. Esposito, P. Viglino, J. Briggs, and J. A. McCammon. 1998. pKa shift effects on backbone amide base-catalyzed hydrogen exchange. *J. Am. Chem. Soc.* 120:3735–3738.

Fowler, R. H., and E. A. Guggenheim. 1939. Statistical Thermodynamics. Cambridge University Press, Cambridge.

Gilson, M. K., M. E. Davis, B. A. Luty, and J. A. McCammon. 1993. Computation of electrostatic forces on solvated molecules using the Poisson-Boltzmann equation. *J. Phys. Chem.* 97:3591–3600.

Gilson, M. K., and B. Honig. 1986. The dielectric constant of a folded protein. *Biopolymers.* 25:2097–2119.

Gilson, M. K., K. A. Sharp, and B. Honig. 1987. Calculating the electrostatic potential of molecules in solution: method and error assessment. *J. Comp. Chem.* 9:327–335.

Gilson, M. K., T. P. Straatsma, J. A. McCammon, D. R. Ripoll, C. H. Faerman, P. H. Axelsen, I. Silman, and J. L. Sussman. 1994. Open "back door" in a molecular dynamics simulation of acetylcholinesterase. *Science.* 263:1276–1278.

Gouy, M. 1910. Sur la constitution de la charge électrique a la surface d'un électrolyte. *Journ. de Phys.* 9:457–468.

Grahame, D. C. 1947. The electrical double layer and the theory of electrocapillarity. *Chem. Rev.* 32:441–501.

Gronwall, T. H., V. K. La Mer, and K. Sandved. 1928. Über den einfluß der sogenannten höheren glieder in der Debye-Hückelschen theorie der lösungen starker elektrolyte. *Physik. Zeitschr.* 29:358–393.

Gueron, M., and G. Weisbuch. 1980. Polyelectrolyte theory. I. Counterion accumulation, site-binding, and their insensitivity to polyelectrolyte shape in solutions containing finite salt concentrations. *Biopolymers.* 19:353–382.

Gueron, M., and J.-P. Demaret. 1992. Polyelectrolyte theory IV. Algebraic approximation for the Poisson-Boltzmann free energy of a cylinder. *J. Phys. Chem.* 96:7816–7820.

Gueron, M., and G. Weisbuch. 1979. Polyelectrolyte theory. 2. Activity coefficients in Poisson-Boltzmann and condensation theory. The polarizability of the counterion sheath. *J. Phys. Chem.* 83:1991–1998.

Honig, B., and A. Nicholls. 1995. Classical electrostatic in biology and chemistry. *Science.* 268:1144–1149.

Hsu, J.-P., and B.-T. Liu. 1996a. Exact solution to the linearized Poisson-Boltzmann equation for spheroidal surfaces. *J. Colloid Interface Sci.* 175:785–788.

Hsu, J.-P., and B.-T. Liu. 1996b. Solution to the linearized Poisson-Boltzmann equation for a spheroidal surface under a general surface condition. *J. Colloid Interface Sci.* 183:214–222.

Jackson, J. D. 1962. Classical electrodynamics, John Wiley and Sons, New York.

Jayaram, B., and D. L. Beveridge. 1996. Modeling DNA in aqueous solutions: theoretical and computer simulation studies on the ion atmosphere of DNA. *Annu. Rev. Biophys. Biomol. Struct.* 25:367–394.

Jorgensen, W. L., and J. Tirado-Rives. 1988. The OPLS potential functions for proteins. Energy minimizations for crystals of cyclic peptides and crambin. *J. Am. Chem. Soc.* 110:1657–1666.

Lifson, S., and A. Katchalski. 1954. The electrostatic free energy of polyelectrolyte solutions. II. Fully stretched macromolecules. *J. Polymer Sci.* 13:43–55.

Katchalski, A. 1971. Polyelectrolytes. *Pure Appl. Chem.* 26:327–371.

Kirkwood, J. G. 1934. Theory of solutions of molecules containing widely separated charges with special applications to zwitterions. *J. Chem. Phys.* 7:351–361.

Madura, J. D., M. E. Davis, M. K. Gilson, R. Wade, B. A. Luty, and J. A. McCammon. 1994. Biological applications of electrostatics calculations and Brownian dynamics simulations. *Rev. Comp. Chem.* 5:229–267.

Madura, J. D., J. M. Briggs, R. Wade, M. E. Davis, B. A. Luty, A. Ilin, A. Antosiewicz, M. K. Gilson, B. Bagheri, L. Ridgway Scott, and J. A. McCammon. 1995. Electrostatics and diffusion of molecules in solution: simulations with the University of Houston Brownian dynamics program. *Comp. Comm. Phys.* 91:57–95.

Marcus, R. A. 1955. Calculation of thermodynamic properties of polyelectrolytes. *J. Chem. Phys.* 23:1057–1068.

McCammon, J. A., and S. Harvey. 1987. Dynamics of Proteins and Nucleic Acids. Cambridge University Press, Cambridge.

Misra, V. K., K. A. Sharp, R. A. G. Friedman, and B. Honig. 1994. Salt effects on ligand-DNA binding: minor groove antibiotics. *J. Mol. Biol.* 238:245–263.

Murthy, C. S., R. J. Bacquet, and P. J. Rossky. 1985. Ionic distributions near polyelectrolytes: a comparison of theoretical approaches. *J. Phys. Chem.* 89:701–710.

Nicholls, A. 1993. GRASP: Graphical representation and analysis of surface properties. Columbia University, New York.

Onsager, L. 1933. Theories of concentrated electrolytes. *Chem. Rev.* 13: 73–89.

Pranata, J. S. G., S. G. Wierschke, and W. L. Jorgensen. 1991. OPLS potential functions for nucleotide bases. Relative association constants of hydrogen-bonded base pairs in chloroform. *J. Am. Chem. Soc.* 113: 2810–2819.

Press, W. H., B. P. Flannery, S. A. Teukolsky, and W. Vetterling. 1990. Numerical Recipes in C, Cambridge University Press, New York.

Ragona, L., F. Pusterla, L. Zetta, H. L. Monaco, and H. Molinari. 1997. Identification of a Conserved Hydrophobic Cluster in Partially Folded β-lactoglobulin at pH 2. *Folding and Design.* 2:281–290.

Reiner, E. S., and C. J. Radke. 1990. Variational approach to the electrostatic free energy in charged colloidal suspensions: general theory for open systems. *J. Chem. Soc. Faraday Trans.* 86:3901–3912.

Rouzina, I., and V. A. Bloomfield. 1996. Competitive electrostatic binding of charged ligands to polyelectrolytes: planar and cylindrical geometries. *J. Phys. Chem.* 100:4292–4304.

Sharp, K. A. 1995. Polyelectrolyte electrostatics: salt dependence, entropic and enthalpic contribution to free energy in the nonlinear Poisson-Boltzmann model. *Biopolymers.* 36:227–243.

Sharp, K. A., and B. Honig. 1990. Calculating total electrostatic energies with the nonlinear Poisson-Boltzmann equation. *J. Phys. Chem.* 94: 7684–7692.

Sharp, K., R. Fine, and B. Honig. 1987. Computer simulation of the diffusion of a substrate to an active site of an enzyme. *Science.* 236: 1460–1463.

Sharp, K. A., A. Jean-Charles, and B. Honig. 1992. A local dielectric constant model for solvation free energies which accounts for solute polarizability. *J. Phys. Chem.* 96:3822–3828.

Sharp, K. A. 1995. Polyelectrolyte electrostatics: salt dependence, entropic and enthalpic contribution to free energy in the nonlinear Poisson-Boltzmann model. *Biopolymers.* 36:227–243.

Stigter, D. 1975. The charged colloidal cylinder with a Gouy double layer. *J. Colloid Interface Sci.* 53:873–879.

Stigter, D. 1978. On the invariance of the charge of electrical double layers under dilution of the equilibrium electrolyte solution. *Progr. Colloid and Polymer Sci.* 65:45–52.

Verwey, E. J. W., and J. Th. G. Overbeek. 1948. Theory of the stability of lyophobic colloids, Elsevier, Amsterdam.

Yoon, B. J., and S. Kim. 1989. Electrophoresis of spheroidal particles. *J. Colloid Interface Sci.* 128:275–288.

Weisbuch, G., and M. Gueron. 1983. Une longueur d'échelle pour les interfaces chargées. *J. Phys.* 44:251–256.

Weisbuch, G., and M. Gueron. 1981. Polyelectrolyte theory. III. The surface potential in mixed-salt solutions. *J. Phys. Chem.* 85:517–525.

Zhou, H.-X. 1994. Macromolecular electrostatic energy within the nonlinear Poisson-Boltzmann equation. *J. Chem. Phys.* 100:3152–3162.